Orig Life Evol Biosph (2011) 41:469–482
DOI 10.1007/s11084-011-9241-6

PREBIOTIC CHEMISTRY

Adsorption of Ribose Nucleotides on Manganese Oxides with Varied Mn/O Ratio: Implications for Chemical Evolution

Brij Bhushan · Uma Shanker · Kamaluddin

Received: 31 March 2011 / Accepted: 20 May 2011 /
Published online: 31 May 2011

Abstract Manganese exists in different oxidation states under different environmental conditions with respect to redox potential. Various forms of manganese oxides, namely, Manganosite (MnO), Bixbyite (Mn_2O_3), Hausmannite (Mn_3O_4) and Pyrolusite (MnO_2) were synthesized and their possible role in chemical evolution studied. Adsorption studies of ribose nucleotides (5′-AMP, 5′-GMP, 5′-CMP and 5′-UMP) on these manganese oxides at neutral pH, revealed a higher binding affinity to manganosite (MnO) compared to the other manganese oxides. That manganese oxides having a lower Mn-O ratio show higher binding affinity for the ribonucleotides indirectly implies that such oxides may have provided a surface onto which biomonomers could have been concentrated through selective adsorption. Purine nucleotides were adsorbed to a greater extent compared to the pyrimidine nucleotides. Adsorption data followed Langmuir adsorption isotherms, and X_m and K_L values were calculated. The nature of the interaction and mechanism was elucidated by infrared spectral studies conducted on the metal-oxide and ribonucleotide-metal-oxide adducts.

Keywords Chemical evolution · Manganese oxides · Ribose nucleotides

Abbreviations

OD	Optical density
P_{ZPC}	Zero point charge
XRD	X-Ray diffraction
TGA	Thermo gravimetric analysis
DTA	Differential thermo analysis
FE-SEM	Field emission scanning electron microscopy
TEM	Transmission electron microscope

B. Bhushan · U. Shanker · Kamaluddin (✉)
Department of Chemistry, Indian Institute of Technology Roorkee, Roorkee 247667 UK, India
e-mail: kamalfcy@iitr.ernet.in

Introduction

Though life that exists today is based on DNA genomes and protein enzymes, there is convincing evidence that hypothesizes the origin of life based on RNA (Joyce and Orgel 1999). This primordial era referred to as the "RNA world" (Gilbert 1986) hypothesizes that all modern organisms are descendants of a prebiotic self-replicating moiety, which utilized RNA as both genetic as well as catalytic material (Srivatsan 2004). This hypothesis is now an almost universally held view (Joyce 2002; Orgel 2004; Gestland et al. 2006); but could this RNA World have stood at the ultimate origin of life? This is currently still an open question. Yet while there are still substantial problems, there are now good leads for simple, spontaneous processes on the early Earth for both the synthesis of nucleotides and their concentration to oligonucleotides.

Further study on the origin of life addressed questions regarding the sources of small organic molecules that composed the first self-replicating system and the mechanism of evolution of cell-like enclosure from an abiotic supply of biomonomers (Lazcano and Miller 1999; Luisi et al. 2004). Numerous chemical and biochemical studies pertaining to the chemical evolution and origin of life, performed under simulated prebiotic conditions, have appeared owing to various pioneering work in this field (Cairns-Smith 1982; Orgel 1998; Miller 1997; Ferris 1993; Schwartz and Orgel 1995) but such aggregation of biological precursors into prebiotic biopolymers was puzzling to many. It was Bernal who proposed that adsorption of organic molecules onto mineral surface like clays would have catalytic relevance to the emergence of prototypical polymeric templates (Bernal 1951). Similarly Ferris showed that clays could catalyze activated nucleotide polymerization reactions (Ertem and Ferris 1997; Ferris et al. 1989; Ferris and Ertem 1992; Ferris and Hagan 1986; Ferris and Kamaluddin 1990). Smith studied the potential role of natural minerals on which aggregation and entrapment of nucleobases might have occurred thereby, reinforcing the potential role of natural minerals acting as scaffolds and aiding in the catalysis of reactions necessary for the evolution of early life (Smith 1998).

Like natural minerals, transition metals may have been important as catalysts for the formation of biopolymers during chemical evolution and the origin of life (Arora and Kamaluddin 2007; Arora et al. 2007; Arora and Kamaluddin 2009). Catalysts may have been important for the origins of life because they tend to direct the reaction along a few reaction pathways so that a limited array of products is obtained. Catalysts bind specific types of compounds to their surfaces and then convert them to a limited number of products. Manganese is the 10^{th} most abundant element in the biosphere ($\sim 10^{14}$ kg of suspended and dissolved manganese found in oceans) and is second only to iron in relative terrestrial abundance of the transition metals. On average, crustal rocks contain about 0.1% by weight of Mn (Turekian and Wedepohl 1961), coordinated with oxygen, and may also exist in the bottom of seas as nodules. The existence of manganese on Mars has also been reported (Heiserman 1992). In the early stages of the Earth's evolution, volcanoes were a major source of such elements which in turn may have been involved in adsorption and catalytic reactions of biomolecules in molecular evolution. The catalytic activity of manganese for many reactions in the presence of nucleotides, mRNA to give oligoribonucleotides is already reported (Hroacki and Hiromichi 1999). Visscher and Schwartz have concluded that the synthesis of pyrophosphate-linked oligomers from the bis-phosphoimidazolides of deoxyadenosine and deoxyguanosine, as well as from acyclic analogs of these nucleosides, is catalyzed much more effectively by Mn (II) (Visscher and Schwartz 1989).

Manganese exists in various oxidation states on Earth. The microbial oxidation of soluble Mn (II) is an important process for the formation of soluble Mn (III, IV) oxides in natural environments (Nealson et al. 1988). Abiotic oxidation of Mn (II) under aerobic condition at neutral pH proceeds only at a limited rate (Tebo et al. 1997; 2004). Microorganisms are responsible for much of the Mn-oxide as they greatly accelerate its formation rate (Nealson et al. 1988) and produce oxidation states of ≥3.4 compared to the abiotic laboratory synthesis value of 3.1 (Tebo et al. 1997).

We proposed that since the redox potential of the primitive Earth's atmosphere was low and the atmosphere was less oxidized, manganese oxides of lower oxidation states were more important for selectively adsorbing and concentrating bio-molecules during chemical evolution. In the present work, we studied the interaction of ribose nucleotides namely, 5′-GMP, 5′-AMP, 5′-CMP and 5′-UMP with manganese oxides of varied Mn/O ratio (MnO, Mn_3O_4, Mn_2O_3 and MnO_2). Ribose nucleotides have negatively charged phosphate groups, lone pair containing nitrogen atoms, and aromatic rings with π electron clouds. So interaction could have taken place with the negatively charged moieties of nucleotide and the positively charged surface of manganese oxides (Yao and Millero 1996; Daou et al. 2007). It was observed through a series of adsorption studies that manganese oxides of lower oxidation state are adsorbents for ribonucleotides and thus may have played a role in chemical evolution.

Experimental

Materials and Method

Manganese acetate (Merck), Ammonium oxalate (Merck), 5′- AMP (Sisco Research Laboratories, Mumbai, India), 5′-GMP (SRL), 5′-CMP (SRL) and 5′-UMP (SRL), were used as supplied. All other chemicals used were of analytical reagent grade.

Preparation of Metal Oxides

Manganese oxides were prepared from manganese oxalate through a reported method (Ahmad and Kandalam 2004). First, we synthesized manganese oxalate from two micro-emulsions (I and II) as described below. In the second step, the manganese oxalate particles were subjected to thermal decomposition to yield manganese oxides. MnO, Mn_2O_3 and Mn_3O_4 were obtained by thermal decomposition of manganese oxalate in vacuum (12 h), air (6 h), and nitrogen (8 h), respectively.

Micro-emulsion **I** is composed of cetyltrimethylammonium bromide (CTAB) as the surfactant, n-butanol as the co-surfactant, isooctane as the hydrocarbon phase and 0.1 M manganese acetate solution as the aqueous phase. Micro-emulsion **II** is comprised of the same constituents as above except for having 0.1 M ammonium oxalate instead of manganese acetate as the aqueous phase. The weight fractions of various constituents in these micro-emulsions are as follows: 16.76% CTAB, 13.90% n-butanol, 59.29% isooctane and 10.05% aqueous phase. These two micro-emulsions were mixed slowly and stirred overnight on a magnetic stirrer, and the resulting precipitate was separated from the apolar solvent and surfactant by centrifuging and washing it with 1:1 mixture of methanol and chloroform. The precipitate was dried in an oven at 120°C for 1 h. The precursors were heated under different conditions to obtain the oxides. The precursor on heating in air at

450°C for 6 h leads to the formation of Mn_2O_3. Under nitrogen at 500°C (8 h) Mn_3O_4 was obtained. MnO was obtained by decomposing manganese oxalate in a sealed quartz tube at a pressure ~10^{-5} torr. The sealed tube was heated slowly to 500°C at the rate of 50°C h^{-1}. It was then annealed for 12 h and then cooled at the rate of 25°C h^{-1}.

Manganese dioxide ($MnO_{2)}$ was prepared as follows: Manganese acetate ($MnAc_2 \cdot 4H_2O$) and citric acid ($C_6H_8O_7 \cdot H_2O$) in a mol ratio 1:2 were dissolved in distilled water (500 ml) in a beaker. The solution was adjusted to pH ~6 by addition of ammonia. Then, the solution was heated to 80°C with a magnetic stirring and kept at this temperature for several hours until a wet gel was obtained. The wet gel was dried at 110°C in a drying box, and a dried gel was obtained. Then the dried gel was calcined at 380°C for 12 h in a muffle furnace. The calcined product was treated with a 2 M aqueous H_2SO_4 solution (50 ml) for 2 h at 80°C with magnetic stirring in order to increase the degree of oxidation of the product. After acid-treatment, the product was rinsed with distilled water and filtered, then dried at 105°C, and finally the brownish black manganese dioxide material was obtained (Xiuling et al. 2007).

Synthesized manganese oxides were ground and sieved through a 100 mesh sieve and were subjected to spectral (1600 series FTIR, Perkin-Elmer and XRD (PW1410/20, Philips Hall) and adsorption studies.

Spectral Studies

The adsorption of 5′-AMP, 5′-GMP, 5′-CMP and 5′-UMP on manganese oxides were studied by measuring absorbance at their characteristic λ_{max} values of 259, 254, 278 and 262 nm, respectively. Absorbance was measured using a Shimadzu UV-1601 UV visible spectrophotometer. The infrared spectra of adsorbents, adsorbate, and adsorption adducts were recorded on KBr discs on a Perkin Elmer 1600 Series Fourier transform infrared spectrophotometer.

BET Surface Area

The BET surface area of the manganese oxides was estimated by using nitrogen adsorption isotherms on micromeritics ASAP 2010 (UK). Samples were activated at 473 K for 4 h prior to the measurement.

Adsorption Studies

The parameters like concentration range of adsorbate, particle size of adsorbent, contact time to attain adsorption equilibrium, quantity of adsorbent, pH and the temperature were fixed to study the adsorption of ribose nucleotides on manganese oxides. Adsorption of nucleotides on manganese oxides was studied with the use of varying concentration of nucleotides (5×10^{-5} M to 6×10^{-4} M). Twenty five milligrams each of the manganese oxides were added to 5 ml of different concentrations of aqueous solution of nucleotide. pH was adjusted by adding 0.01 M acid (HCl) or base (NaOH). Mixtures were shaken for about 2 min on Vortex shaker (Spinix) and kept at room temperature for 24 h. The mixture after 24 h was centrifuged on REMI R4C centrifuge for 35 min at 4,500 rpm. Absorbance of the supernatant was measured at the characteristic λ_{max} of the nucleotide. The concentration of

nucleotides after adsorption for 24 h was determined with the help of calibration curve made by plotting concentration vs. optical density (O. D.) of nucleotide standard solutions. The amount of nucleotide adsorbed was calculated using the absorbance of nucleotide before and after adsorption. The nucleotide- manganese adducts were washed with water, dried, and subjected to IR studies.

Field Emission Scanning Electron Microscope Studies

FE-SEM images of adsorbent, adsorbate and adduct were taken using Scanning Electron Microscope FEI Quanta 200F microscope operating at an accelerating voltage of 20 kV. Using FE-SEM, we imaged the surface morphology of the metal oxides, nucleotides and metal oxide-nucleotide adducts.

Transmission Electron Microscopy Studies

TEM images of metal oxides were recorded by Transmission Electron Microscope (FEI TECNAI G2 microscope operating at 200 kV.).

Results

Manganese oxalate dihydrate was characterized by powder X-ray diffraction. The data obtained is shown in (Fig. 1). This revealed good agreement with JCPDS (Joint Committee on Powder Diffraction Standards) (32–0647). TGA (Thermal Gravimetrical Analysis) curve of manganese oxalate shown in (Fig. 2) has two major changes occurring at 120°C (removal of two water molecules) and at 300°C (unhydrated manganese oxalate changing into their oxides) (Ahmad and Kandalam 2004). Synthesized manganese oxides were characterized by powder XRD, FE-SEM and TEM techniques. Powder XRD reveals that all

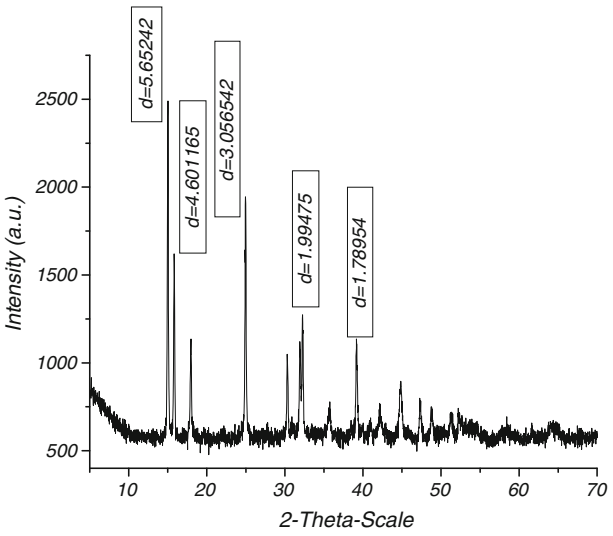

Fig. 1 X- Ray diffraction patterns of manganese oxalate (Mn $(C_2O_4).2H_2O$)

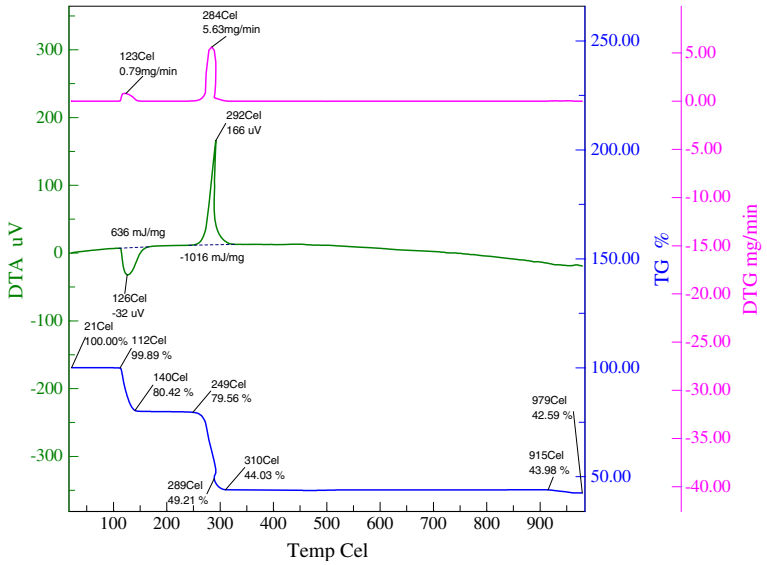

Fig. 2 TGA/DTA of manganese oxalate

Fig. 3 X- Ray diffraction patterns of manganese oxide (**a**) MnO, (**b**) Mn_3O_4, (**c**) Mn_2O_3 and (**d**) MnO_2

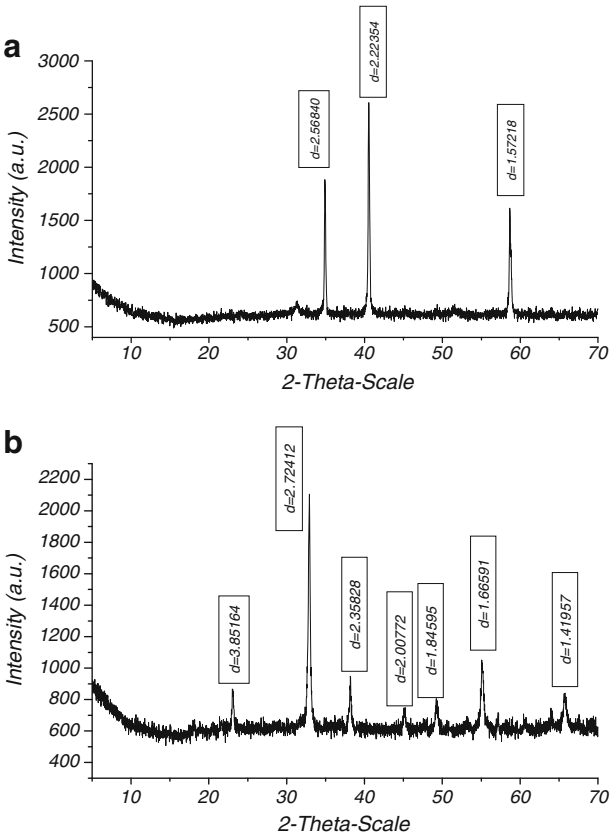

Fig. 3 (continued)

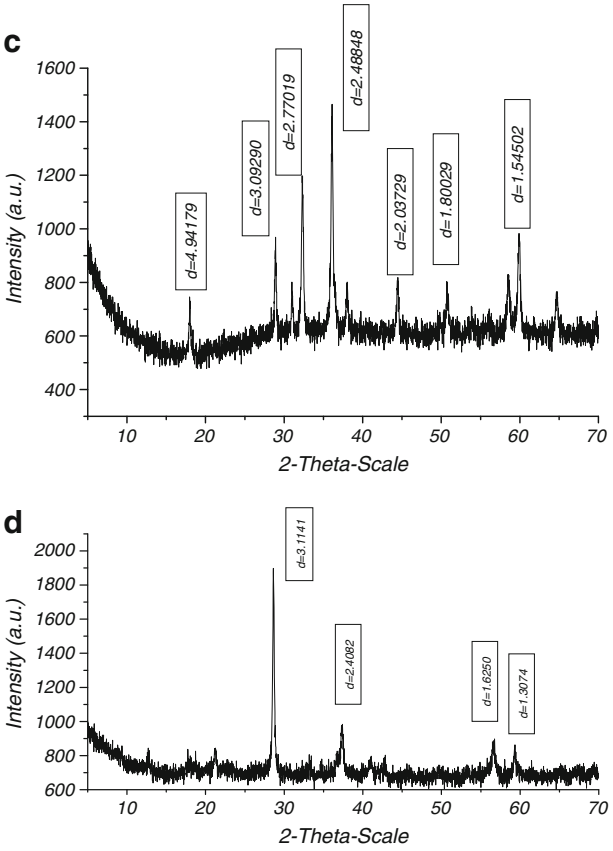

four oxides viz. manganosite (MnO) (Fig. 3a) JCPDS (75–0257), hausmannite (Mn_3O_4) (Fig. 3b) JCPDS (80–0382), bixbyite (Mn_2O_3) (Fig. 3c) JCPDS (76–0150), and pyrolusite (MnO_2) (Fig. 3d) JCPDS (81–2261), have good agreement with JCPDS XRD patterns. Table 1 depicts the specific surface areas of the synthetic manganese oxides which all had more or less similar values. TEM images of the manganese oxides show a spherical, nanotube and nanorod type structure with sizes ranging from 50 to 200 nm (Fig. 4a, b, c and d). FE-SEM images show the surface morphology of manganese oxides before and after adsorption as shown in Fig. 5a, b and c, (a): MnO, (b): 5′- GMP, (c): (MnO + 5′- GMP) adduct. Summarily, FE-SEM images confirm the adsorption of nucleotide on the MnO, Mn_3O_4 and Mn_2O_3 metal surface, while much less adsorption is observed on the MnO_2 surface.

Table 1 Surface area of manganese oxides

Metal oxides	Surface area (m^2/g)
MnO	238.89
Mn_3O_4	226.56
Mn_2O_3	218.35
MnO_2	214.57

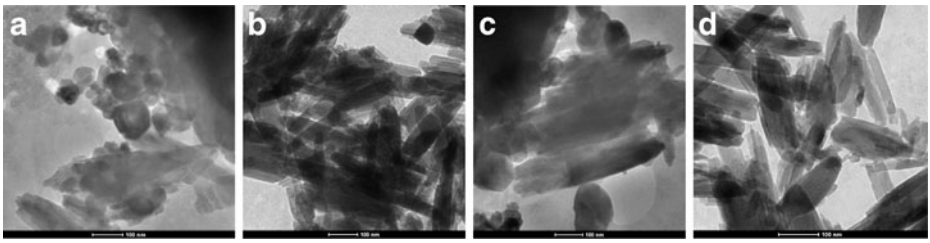

Fig. 4 TEM Images of Manganese Oxides (**a**): MnO, (**b**): Mn_3O_4 (**c**): Mn_2O_3 and (**d**)MnO_2

Adsorption of nucleotides on manganese oxides was studied over a range of concentrations at neutral pH (~7.0). Adsorption isotherms were obtained by plotting the amount of nucleotide adsorbed, X_e (mol/g), versus their equilibrium concentration, C_e (mol L^{-1}). Plots were made in Microsoft Excel. From the adsorption isotherm, the percent adsorption of the nucleotides on the manganese oxides was determined; this data is reported in (Table 2). Percent binding was calculated from absorbance values of nucleotides before and after adsorption at the point of the curve when saturation starts. The initial portion of the isotherms shows a linear relationship between the amount adsorbed and equilibrium concentration. At the higher concentration range, saturation phenomenon was observed (Fig. 6a, b, c and d). The adsorption data were fitted in Langmuir adsorption isotherm (Atkins and de Paul 2002) as given below.

$$\frac{Ce}{X_e} = \frac{Ce}{X_m} + \frac{1}{X_m} k_L$$

Where C_e is equilibrium concentration of nucleotide (mole/liter), X_e is amount (in mol) of nucleotide adsorbed per gram weight of adsorbent, X_m is amount of nucleotide adsorbed at saturation (mol/g), and k_L is Langmuir adsorption constant (L/mol). A typical graph of C_e/X_e vs. C_e is a straight line (Fig. 7a, b, c and d). From the graph, X_m and k_L values were calculated and shown in Table 3. X_m value indicates the maximum amount of nucleotide adsorbed on oxides for monolayer formation; k_L value is related to the enthalpy of adsorption (Atkins and de Paul 2002). The infrared spectra of adenosine monophosphate, manganese oxide, and the manganese –nucleotide adduct are shown in Table 4.

Discussion

Adsorption results depicted in (Table 2) suggest that maximum adsorption of ribonucleotide occurred on the surface of manganosite (MnO), hausmannite (Mn_3O_4) and bixbyite

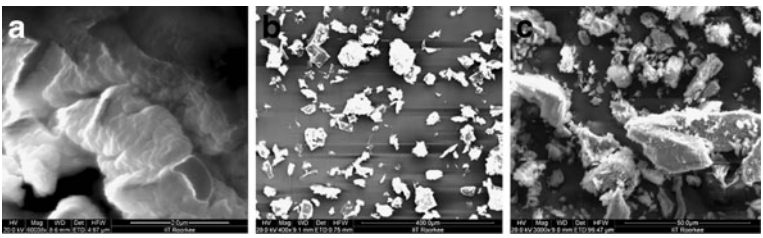

Fig. 5 FE-SEM images of nucleotides, manganese oxides and adduct (**a**): 5′-GMP, (**b**): MnO before adsorption, (**c**): MnO after adsorption

Table 2 Percent binding of nucleotides on manganese oxides at neutral pH and $C_o=40\times10^{-5}$M

Ribose nucleotide	MnO	Mn_3O_4	Mn_2O_3	MnO_2
5′-GMP	79.06	66.79	55.42	33.03
5′-AMP	63.69	53.52	39.87	18.36
5′-CMP	52.18	37.06	20.39	12.06
5′-UMP	36.91	27.46	11.27	2.50

(Mn_2O_3) while less adsorption was observed for pyrolusite (MnO_2). This is further confirmed by the FE-SEM images (Fig. 5). The nanosized particles as evident from the TEM images of the oxides (Fig. 4) and more or less equal surface area of the oxides (Table 1) reveals that the surface of all oxides are conducive for adsorption of ribonucleotide.

The nature of interaction between the ribonucleotide and the oxide plays a vital role in understanding the mechanism underlying the higher adsorption affinity on certain oxides of manganese (Stumm et al. 1970; Parks and De Brum 1962; De Bruyn and Agar 1962; Bepuee and De Brvy 1968; Atkinson et al. 1967). In a manganese oxide/water system, Me-OH_2^+ and Me-O^{-1}, hydroxyl groups on the solid surface are the most important sites for surface interactions. These groups can act as acids or bases, depending on the pH of the solution. In the present study, according to the literature (Kosmulski 2002; Kosmulski 2004; Kosmulski 2006; Healy et al. 1966), the zero points of charge P_{ZPC} of MnO, Mn_2O_3, Mn_3O_4 and MnO_2 are >10, >10, 7.7 and 7.3 respectively. At neutral pH ($pH<P_{ZPC}$), the hydroxyl groups on the manganese oxide surface exist in the

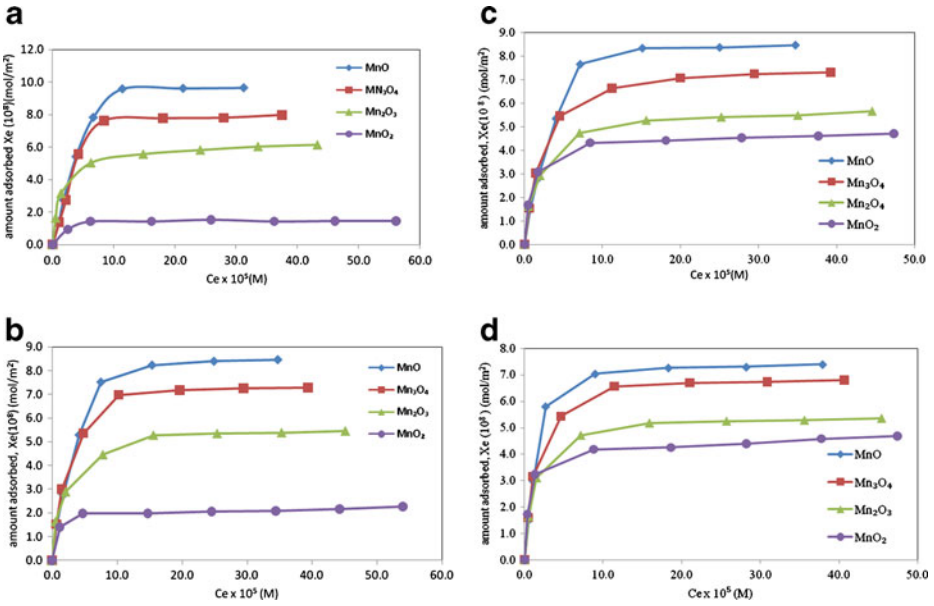

Fig. 6 Adsorption isotherm of nucleotides on manganese oxides: (**a**): 5′-GMP, (**b**): 5′-AMP, (**c**): 5′-CMP, (**d**): 5′-UMP

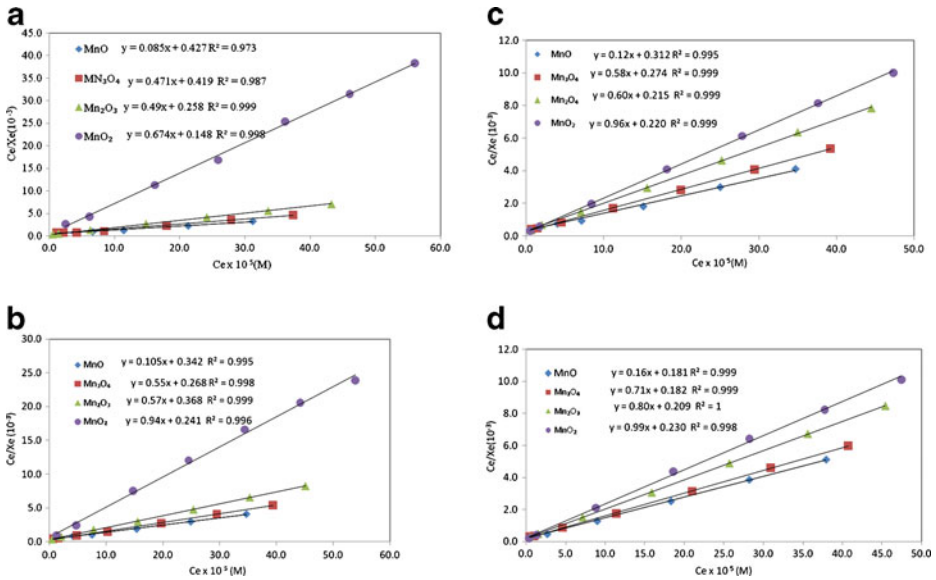

Fig. 7 Langmuir isotherm plots for nucleotides on manganese oxides: (**a**): 5′-GMP, (**b**): 5′-AMP, (**c**): 5′-CMP, (**d**): 5′-UMP

acidic form and the adsorbent surface is positively charged. Electrostatic interactions of positively charged surface of manganese oxides (MnO and other manganese oxides) with nucleotides may take place through negatively charged atoms in the phosphate groups, via the π electrons of the aromatic ring or rings, and/or via the lone pair of electrons on N and O atoms. Such explanations are verified by the infrared spectral studies conducted.

The nature of the interaction between ribonucleotides and the manganese oxides is mainly electrostatic, which was further elucidated by means of infrared absorption study which showed shifting of particular metal oxide-phosphate peaks (Daou et al. 2007; Antelo et al. 2005; Chitrakar et al. 2006; Li and Stanforth 2000). Electrostatic interaction of phosphate groups with positively charged groups and hydroxyl sites at the surface of magnetite was postulated by Daou et al. Antelo et al. similarly stressed the importance of pH and ionic strength while explaining the higher adsorption of phosphate to goethite in acidic medium. Higher adsorption of phosphate by goethite at acidic pH was also explained by Chitrakar et al. and Li and Stanforth in lines of electrostatic forces of attraction as the primary mode of interaction. The shift in wavelengths of characteristic frequencies of ribonucleotides in nucleotide-manganese adducts (Table 4) indicates interactions between

Table 3 Langmuir constants ($k_L \times 10^{-3}$) in L/mol for adsorption of nucleotides on manganese oxides ($Xm \times 10^8$) mol/m^2 values in bracket

Ribose nucleotide	MnO	Mn_3O_4	Mn_2O_3	MnO_2
5′-GMP	5.023 (11.76)	0.891 (2.13)	0.526 (2.04)	0.301 (1.48)
5′-AMP	3.257 (9.52)	0.487 (1.82)	0.454 (1.80)	0.256 (1.06)
5′-CMP	2.600 (8.33)	0.472 (1.72)	0.385 (1.67)	0.229 (1.04)
5′-UMP	1.117 (6.17)	0.256 (1.41)	0.261 (1.20)	0.215 (1.01)

Table 4 Typical infrared spectral frequencies (cm^{-1}) of ribonucleotides before and after absorption on manganese oxide

Ribonucleotides	υ_{NH_2}		δ_{NH}	$\nu_{C\text{-}O\text{-}P}$
5′-AMP	3221 (3382)[a]	3343 (3439)	1647 (1629)	1084 (1102)
5′-GMP	3143 (3329)	3433 (3440)	1605 (1638)	1083 (1104)
5′-CMP	3122 (3342)	3334 (3436)	1539 (1421)	1091 (1160)
5′-UMP	1473 (1384)	1082 (1127)		

[a] Bracket values are after adsorption

the ribonucleotides and manganese. It appears that the binding may also be mediated by either N-1 or N-7 for 5′GMP and 5′AMP, and N-3 for 5′CMP and 5′UMP. The adsorption is presumably related to the involvement of N-1, N-3 and N-7 of the base residues, lone pair of nitrogen atom, and to the dissociation of the two available protons of the phosphate groups. A shift towards lower wavelength of N-H bending from 1,647 cm^{-1} to 1,629 cm^{-1} shows the involvement of the NH_2 groups present on the base of 5′GMP ribonucleotides in the interaction of ribonucleotides with manganese. A strong band at 1,084 cm^{-1} in 5′GMP corresponding to C-O-P vibration has been shifted to 1,102 cm^{-1}. Thus interaction likely takes place through amino and phosphate groups of ribonucleotides with positively charged manganese oxide surfaces (Arora and Kamaluddin 2009).

The presence of significant change in the typical infrared frequencies of N-H and C-O-P suggests that the adsorption of ribonucleotides is a surface phenomenon occurring on the surface of metal oxides. Ribonucleotides interact through their purine or pyrimidines residue and phosphate group with the positively charged surface of the mineral. Greater adsorption of 5′-GMP and 5′-AMP may be due to the higher number of π electrons in their aromatic ring system.

Manganese oxides with different oxidation states like 2, 3 and 4 exist (Bish and Post 1988; Burns et al. 1985; De Guzman et al. 1993; Shen et al. 1992) with decreasing average volume per Mn ion (A^3) in each form of the oxide (Li and Stanforth 2000). The prebiotic condition existing in the bottom of sea was essentially reducing (Wachtershauser 1988). This is suitable for the adsorption of ribonucleotides on the surface of the Mn (II) and Mn (III) which changed slowly to the more stable state of manganese oxide, Mn (IV) with the increasingly oxidizing nature of the primitive Earth's atmosphere (Jortner 2006). The oxic conditions prevailing at bottom of seas were clarified by thallium isotope studies carried out by Nielson (Nielsen et al. 2006) and further reported by Sleep and Bird (Sleep and Bird 2008).

At neutral pH the adsorption of 5′-GMP was the greatest of all the ribonucleotides with all of the oxides studied (Table 2). In general, MnO and Mn_3O_4 oxides of manganese were found to have an extremely high affinity toward ribonucleotides as the extent of surface covered $(\theta = kLCe/1 + kLCe)$ was determined to be about maximum (~100%). Purine nucleotides (5′GMP and 5′AMP), which have one more ring and a lone pair of electrons at the N-7 position, are adsorbed more strongly on manganese oxides than are the pyrimidine nucleotides (5′CMP and 5′UMP).

Conclusion

All of the manganese oxides synthesized from manganese oxalate were nanosized, their surface morphology was irregular and porous, and all had more or less similarly high

specific surface areas. All these observations are favorable and conducive to higher adsorption of ribose nucleotides. Our studies also revealed that nucleotides have a greater binding affinity on lower oxidation state manganese oxides (MnO and Mn_3O_4). Adsorption was higher for 5′-GMP and 5′-AMP compared to 5′-CMP and 5′-UMP. We conclude that electrostatic interactions are likely the main contributing factors for the observed adsorption on manganese (II) and (III) oxides. The higher electrostatic interaction between the positive metal-oxide surface and the negative part of the ribonucleotide could have been conducive for adsorption and preservation of these biomolecules as well as for promoting further polymerization reactions.

Acknowledgement We are thankful to Indian Space Research Organization (ISRO), Bangalore, India, for financial support.

References

Ahmad T, Kandalam V (2004) Nanorods of manganese oxalate: single source precursor to different manganese oxide nanoparticles (MnO, Mn_2O_3, Mn_3O_4). J Mater Chem 14:3406–3410

Antelo J, Avena M, Fiol S, Lopez R, Arce F (2005) Effects of pH and ionic strength on the adsorption of phosphate and arsenate at the goethite–water interface. J Colloid Interface Sci 285:476–486

Arora AK, Kamaluddin (2007) Interaction of ribose nucleotides with zinc oxide and relevance in chemical evolution. Colloids surf A Physicochem Eng Asp 298:186–191

Arora AK, Kamaluddin (2009) Role of metal oxides in chemical evolution: interaction of ribose nucleotides with alumina. Astrobiol 9:165–171

Arora AK, Tomar V, Aarti VKT, Kamaluddin (2007) Hematite–Water system on Mars and its possible role in chemical evolution. Int J Astrobiol 6:267–271

Atkins P, de Paul J (2002) Atkins' physical chemistry, 7th edn. Oxford University Press, Oxford

Atkinson RJ, Posner AM, Quirk JP (1967) Adsorption of potential determining ions at the ferric oxide-aqueous electrolyte interface. J Phys Chem 71:550–558

Bepuee YG, De Brvy PL (1968) Adsorption at the rutile-solution interface: I. Thermodynamic and experimental study. J Colloid Interface Sci 27:305–318

Bernal JD (1951) The physical basis of life. Routledge and Kegan Paul, London

Bish DL, Post JE (1988) Rietveld refinement of the todorokite structure. Am Mineral 74:861–869

Burns RG, Burns VM, Stockman HW (1985) The todorokitebuserite problem: further considerations. Am Mineral 70:205–208

Cairns-Smith AG (1982) Genetic takeover: and the mineral origins of life. Cambridge University Press, New York

Chitrakar R, Tezuka S, Sonoda A, Sakane K, Ooi K, Hirotsu T (2006) Phosphate adsorption on synthetic goethite and akaganeite. J Colloid Interface Sci 298:602–608

Daou TJ, Begin-Colin S, Greneche JM (2007) Phosphate adsorption properties of magnetite-based nanoparticles. Chem Mater 19:4494–4505

De Bruyn PL, Agar GE (1962) In: Fuerstenau DW (ed) Froth flotation. AIME, New York

De Guzman RN, Shen YF, Shaw BR, Suib SL, O'young CL (1993) Role of cyclic voltammetry in characterizing solids: natural and synthetic manganese oxide octahedral molecular sieves. Chem Mater 5:1395–1400

Ertem G, Ferris JP (1997) Template-directed synthesis using the heterogeneous templates produced by montmorillonite catalysis. A possible bridge between the prebiotic and RNA worlds. J Am Chem Soc 119:7197–7201

Ferris JP (1993) Catalysis and prebiotic RNA synthesis. Origins. Orig Life Evol Biosph 5:307–315

Ferris JP, Ertem G (1992) Oligomerization of ribonucleotides on montmorillonite: reactions of the 5 – phosphorimidazolide of adenosine. Science 257:1387–1389

Ferris JP, Hagan WJ (1986) Adsorption and reaction of adenine nucleotide on montmorillonite. Orig Life Evol Biosph 17:69–84

Ferris JP, Kamaluddin EG (1990) Oligomerization reactions of deoxyribonucleotides on montmorillonite clay: the effect of mononucleotide structure, phosphate activation and montmorillonite composition on phosphodiester bond formation. Orig Life Evol Biosph 20:279–291
Ferris JP, Ertem G, Agarwal VK (1989) The adsorption of nucleotides and polynucleotides on montmorillonite clay. Orig Life Evol Biosph 19:153–164
Gestland RF, Cech TR, Atkins JF (2006) The RNA world. Cold Spring Harbour Laboratory Press, Cold Spring Harbour
Gilbert W (1986) Origin of life: the RNA world. Nature 319:618
Healy TW, Herring AP, Fuerstenau DW (1966) The effect of crystal structure on the surface properties of a series of manganese dioxides. J Colloid Interface Sci 21:435–444
Heiserman DL (1992) Exploring chemical elements and their compounds. Blue Ridge Summit, PA Libraries, Australia
Hroacki S, Hiromichi W (1999) Synthesis and reaction of nucleoside 5- diphosphate imidazolide: a nonenzymatic capping agent for 5-monophosphorylated oligoribonucleotides in aqueous solution. J Org Chem 64:5836–5840
Jortner J (2006) Conditions for the emergence of life on the early Earth: summary and reflections. Phil Trans R Soc B 361:1877–1891
Joyce GF (2002) The antiquity of RNA based evolution. Nature 418:214–221
Joyce GF, Orgel LE (1999) "Prospects for understanding the origin of the RNA world." In the RNA world, 2nd edn. Cold Spring Harbor Laboratory Press, Cold Spring Harbor, pp 49–77
Kosmulski M (2002) pH-Dependent surface charging and points of zero charge. J Colloid Interface Sci 253:77–87
Kosmulski M (2004) pH-Dependent surface charging and points of zero charge II. Update. J Colloid Interface Sci 275:214–224
Kosmulski M (2006) pH-Dependent surface charging and points of zero charge III. Update. J Colloid Interface Sci 298:730–741
Lazcano A, Miller SL (1999) The stepwise evolution of early life driven by energy conservation. J Mol Evol 49:424–431
Li L, Stanforth R (2000) Distinguishing adsorption and surface precipitation of phosphate on goethite (α-FeOOH). J Colloid Interface Sci 230:12–21
Luisi PL, Rasi PS, Mavelli F (2004) A possible route to prebiotic vesicle reproduction. Artif Life 10:297–308
Miller SL (1997) Peptide nucleic acids and prebiotic chemistry. Nat Struct Biol 4:167–169
Nealson KH, Tebo BM, Rosson RA (1988) Occurrence and mechanisms of microbial oxidation of manganese. Adv Appl Microbiol 33:279–318
Nielsen SG, Rehkamper M, Norman MD, Halliday AN, Harrison D (2006) Thallium isotopic evidence for ferromanganese sediments in the mantle source of Hawaiian basalts. Nature 439:314–317
Orgel LE (1998) The origin of life—a review of facts and speculations. Trends Biochem Sci 23:491–495
Orgel LE (2004) Prebiotic chemistry and the origin of the RNA world. Crit Rev Biochem Mol Biol 39:99–123
Parks GA, De Brum PL (1962) The zero point of charge of oxides. J Phys Chem 66:967–973
Schwartz AW, Orgel LE (1995) Template-directed synthesis of novel, nucleic acid-like structures. Science 228:585–587
Shen YF, Zerger RP, Suib McCurdy L, Potter DI, O'Young CL (1992) Octahedral molecular sieves: preparation, characterization and applications. J Chem Chem Commun 17:1213–1214
Sleep NH, Bird DK (2008) Evolutionary ecology during the rise of dioxygen in the Earth's atmosphere. Phil Trans R Soc B 363:2651–2664
Smith JV (1998) Biochemical evolution. I. Polymerization on internal, organophilic silica surfaces of dealuminated zeolites and feldspars. Proc Natl Acad Sci USA 95:3370–3375
Srivatsan SG (2004) Modeling prebiotic catalysis with nucleic acid-like polymers and its implications for the proposed RNA world. Pure Appl Chem 76:2085–2099
Stumm W, Huang CP, Jenkins SR (1970) Specific chemical interaction affecting the stability of dispersed systems. Croat Chem Acta 42:223–245
Tebo BM, Ghiorse WC, Van Waasbergen LG, Siering PL, Caspi R (1997) Bacterially mediated mineral formation: insights into manganese (II) oxidation from molecular genetics and biochemical studies. Rev Mineral 35:225–266
Tebo BM, Bargar JR, Clement B (2004) Manganese bioxides: properties and mechanisms of formation. Annu Rev Earth Planet Sci 32:287–328

Turekian KK, Wedepohl KL (1961) Distribution of the elements in some major units of the Earth's crust. Geol Soc Am Bull 72:275–192

Visscher J, Schwartz AW (1989) Manganese-catalyzed oligomerizations of nucleotide analogs. J Mol Evol 29:284–287

Wachtershauser G (1988) Before enzymes and templates: theory of surface metabolism. Microbiol Rev 52:452–484

Xiuling Wang, Yuan A, Wang Y (2007) Supercapacitive behaviors and their temperature dependence of sol–gel synthesized nanostructured manganese dioxide in lithium hydroxide electrolyte. J Power Source 172:1007–1011

Yao W, Millero FJ (1996) Adsorption of phosphate on manganese dioxide in seawater. Environ Sci Technol 30:536–541